

NATIONAL AERONAUTICAL ESTABLISHMENT

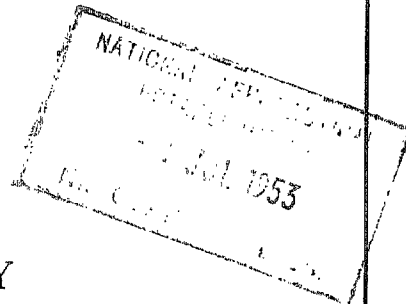
LONDON, ENGLAND

N.A.E.

R. & M. No. 2689

(11,743)

A.R.C. Technical Report



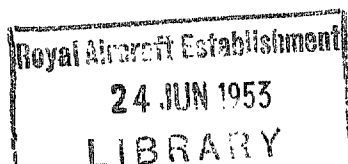
MINISTRY OF SUPPLY

AERONAUTICAL RESEARCH COUNCIL  
REPORTS AND MEMORANDA

High-Speed Tunnel Tests of a  
5 per cent. Chord Dive-Recovery  
Flap on a NACA 0015 Aerofoil

By

D. A. CLARKE, B.Sc.(Eng.), A.C.G.I.



*Crown Copyright Reserved*

LONDON: HER MAJESTY'S STATIONERY OFFICE

1953

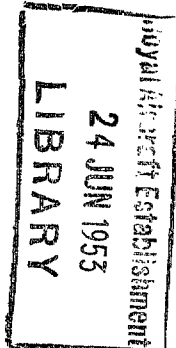
PRICE 5s 6d NET

# High-Speed Tunnel Tests of a 5 per cent. Chord Dive-Recovery Flap on a NACA 0015 Aerofoil

By

D. A. CLARKE, B.Sc.(Eng.), A.C.G.I.

COMMUNICATED BY THE PRINCIPAL DIRECTOR OF SCIENTIFIC RESEARCH (AIR),  
MINISTRY OF SUPPLY



---

*Reports and Memoranda No. 2689\**

*June, 1948*

---

**SUMMARY.**—Pressure plotting tests were made in the Royal Aircraft Establishment High Speed Tunnel on a parallel wooden NACA 0015 wing with dive-recovery flap. The Mach number was varied between 0·30 and 0·80, and the Reynolds number was kept constant at  $1\cdot4 \times 10^6$ .

All combinations of the following were tested :—flap position  $0\cdot2c$ ,  $0\cdot3c$ ,  $0\cdot4c$ ; flap angle 20 deg, 40 deg, incidence 0 deg, 4 deg. The flap-chord/wing-chord ratio was 0·05.

The report presents a general picture of the action of a dive-recovery flap on a wing. The data are, however, too limited to permit the formulation of general design recommendations.

**1. Introduction.**—Little is known about the effects of Mach number, chordwise position, angle, etc., on the action of dive-recovery flaps. The present tests were designed to make a preliminary investigation into the details of this problem.

A part-span flap was mounted on a wing spanning the tunnel, and pressures were measured at the midspan of the flap.

The tests were made in the Royal Aircraft Establishment High Speed Tunnel during August, 1946.

**2. Experimental Details.**—A 15-in. chord NACA 0015 teak wing was mounted vertically, spanning the working-section. A brass flap, with a chord of  $\frac{3}{4}$  in. extended over the middle 3 ft of the span. The gap between flap and wing was sealed with Plasticine.

Pressures were measured at a section midway along the flap, at ten holes on each side of the wing, three on the front surface of the flap and one on the back. Details of the positions are given in Table 3 and Fig. 1.

The wing had been used in previous tests and was slightly warped. This and a residual angle of flow in the tunnel were responsible for differences in pressure at nominal zero incidence between the two sides of the wing without flap (Figs. 3 and 4).

---

\* R.A.E. Report Aero. 2269, received 28th August, 1948.

3. *Range of Tests.*—Tests were made at Mach numbers of 0·3, 0·6, 0·7, 0·74, 0·76, 0·78, 0·80, and at  $\alpha = 0$  deg,  $M = 0\cdot82$  was included. Throughout the tests the Reynolds number was  $1\cdot4 \times 10^6$ . The following cases were tested

Case	Flap Position ( $x_f/c$ )	Flap Angle $\varphi$ (deg)	Incidence $\alpha$ (deg)
A	No Flap		
B	0·4	40	0
C	0·4	20	
D	0·3	40	
E	0·3	20	
F	0·2	40	
G	0·2	20	
H	No Flap		4
J	0·4	40	
K	0·4	20	
L	0·3	40	
M	0·3	20	
N	0·2	40	
P	0·2	20	

The flap-chord/wing-chord ratio was 0·05.

4. *Method of Computation.*—The pressures on the aerofoil surface were integrated to give the normal force and pitching moment about the quarter-chord point, and the pressures on the flap to give normal force on the flap and the moment about the hinge. These four quantities were then compounded to give the total normal force and pitching moment. In every case the pressure on the back of the flap was assumed constant to the flap trailing edge.

The normal force was resolved through the measured angle of incidence to obtain the lift force. The longitudinal component was neglected.

5. *Corrections.*—Tunnel-constraint correction to pitching-moment coefficient amounted to less than 0·002 in the worst case and, therefore, it was not applied. The change of tunnel-constraint correction to local incidence due to putting on the flap amounted to about 0·5 deg in the worst case. No correction has been applied and all comparisons have been made at the same measured incidence.

The same blockage corrections<sup>1</sup> have been applied in all cases. At  $M = 0\cdot80$  the correction to Mach number was 0·01.

6. *Presentation of Results.*—Owing to the amount of computation involved, the results have been worked out only at  $M = 0\cdot74$  and above—apart from a few values at lower Mach numbers. Table 4 gives all the lift and pitching-moment coefficients from  $M = 0\cdot74$  to the highest  $M$  tested. Table 5 gives the normal flap force and hinge-moment coefficients over the same Mach number range. Tables 6 to 9 give pressure coefficients at  $M = 0\cdot76$  and  $0\cdot80$ .

The following information is presented graphically

Fig. 2. Typical change of pressure distribution with  $M$ .

Fig. 3 to 6. Aerofoil pressure distributions at  $M = 0\cdot76$ .

Fig. 7 to 11. Total lift and pitching-moment coefficients.

Fig. 12. Suction behind flap.

Fig. 13 and 14. Chordwise position about which  $\Delta C_M = 0$ .

Fig. 15 to 18. Flap forces and hinge-moment coefficients.

7. *Discussion.*—The graphs of pressure distribution do not include the pressures on the flap, but the contributions of these to the total  $C_L$  and  $C_M$  up to  $M = 0.80$  are in general small, and may be ignored when considering qualitatively the changes in  $C_L$  and  $C_M$  due to the flap or Mach number.

A typical example of the pressure distribution over the aerofoil for a range of Mach numbers is given in Fig. 2. As might be expected, a flap on the lower surface causes an increase in velocity over the upper surface, and hence, at the higher Mach numbers, an increase in the supersonic region and a backward movement of the shock. Except for small flap angles, a region of constant pressure extending to the trailing edge is produced behind the flap at the highest Mach numbers. On the aerofoil with flap the changes of  $C_L$  and  $C_M$  with  $M$  are similar in character to, but larger than, those on a normal aerofoil at incidence.  $C_L$  first increases up to a value of  $M$  between 0.7 and 0.8 : this value depending on flap angle and wing incidence. The rise is checked by a rapid increase in the suction behind the flap (Fig. 12), which continues up to the highest  $M$  reached. As, in addition, the suction coefficients over most of the upper surface begin to fall,  $C_L$  decreases rapidly. Changes in  $C_M$  are small up to  $M = 0.7$ . At higher speeds there is a rapid reduction due to the backward movement of the shock on the upper wing surface, followed at  $\alpha = 0$  deg by an increase as the suction behind the flap rises.

Two American tests on a NACA 10 per cent thick section suggest that in practice these changes in  $C_M$  may be less severe, for whereas two-dimensional tests show reduction in  $C_M$  similar to those in the present test, when a corresponding section with a 20 per cent semispan flap is used for a wing of aspect ratio 9,  $C_M$  rises up to a Mach number of 0.83 and does not fall to its low speed value until a Mach number of 0.90.

Moving the flap forward on the wing has little effect on  $C_L$  and  $C_M$  at zero incidence, but at  $\alpha = 4$  deg at high  $M$  it reduces  $C_L$  and increases  $C_M$ . This effect is due partly to the changed distribution on the lower surface and partly to the forward movement of the shock on the upper surface with forward movement of the flap.

Increasing the flap angle from 20 to 40 deg in general increases  $C_L$  and decreases  $C_M$ .

In most cases at high  $M$  an increase of incidence from 0 deg to 4 deg reduces the increments of  $C_L$  and ( $-C_M$ ).

8. *Application to Complete Aircraft.*—It can be seen that in the range  $M = 0.7$  to 0.8 the lift increment  $\Delta C_L$  due to the flaps is positive and usually above its low speed value, but that  $\Delta C_M$  about the quarter-chord point is negative for nearly all flap angles and positions. On aircraft with tailplanes the increased lift over the flapped portion of the wing is usually in front of the tail and the increased downwash causes a nose-up moment due to the tail<sup>2,3</sup>. This more than counteracts a possible negative moment increment on the wing, and pulls the aircraft out of the dive. The present tests show that at  $M = 0.8$ ,  $\Delta C_L$  is decreasing with  $M$ . Other tests<sup>6</sup> on an 18 per cent thick wing have shown that at still higher Mach numbers  $\Delta C_L$  may fall to zero. Although this effect may be partly due to the high thickness-ratio, it is possible that a similar reduction in  $\Delta C_L$  would occur for a thinner section at a higher speed, making the dive-recovery flap useless at a Mach number of about 0.90 to 0.95.

A flap on a tailless aircraft is ineffective unless it produces a nose-up pitching moment on the wing. Figs. 13 and 14 show the variation with Mach number of  $(x_0/c)$ , where  $(x_0/c)$  is defined as the distance from the leading edge to the point about which  $\Delta C_M$  is zero, *i.e.*, the centre of pressure of the lift increment produced by the flap. For aircraft of about neutral stability, this point must be ahead of the c.g. to produce a positive  $\Delta C_M$  about the c.g. These values of  $(x_0/c)$  give some indication of the difficulty of selecting a suitable flap when the aircraft is tailless, the advisability of keeping the flap as far inboard as possible and of keeping its span fairly low if the wing is sweptback at the body.

Certain model tests have illustrated these difficulties, but they do not agree in detail with these two-dimensional tests. For instance,  $(x_0/c)$  was found to increase with forward movement of the flap. This indicates the need for caution in generalising from the limited results reported here.

9. *Conclusions*.—These tests show that for a flap forward on the lower surface of a wing,  $\Delta C_M$  increases up to a Mach number between 0·7 and 0·8, but the pitching-moment increment (referred to the quarter-chord point) of such a flap usually becomes negative. On aircraft with tails it is known that when the flap is in front of the tail, this decrease in  $C_M$  is usually more than balanced by the increase due to the increased down-wash over the tail. On tailless aircraft, however, it is likely to be very difficult to find a position for the flap which will give a nose-up moment.

At high Mach numbers ( $M > 0\cdot9$ ) it is probable that the lift increment falls to zero, making the flap useless even for an aircraft with a tail.

---

## REFERENCES

No.	Author	Title, etc.
1.	A. Thom .. .. ..	Blockage Corrections and Choking in the R.A.E. High Speed Tunnel. R. & M. 2033. November, 1943.
2.	E. P. Bridgland .. .. ..	Flight Tests of Dive Recovery Flaps on a Single Engine Low Wing Mono-plane ( <i>Thunderbolt</i> ). R.A.E. Tech. Note No. Aero. 1704. October, 1945.
3.	C. M. Britland .. .. ..	High Speed Wind Tunnel Tests on Dive-Recovery Flaps for a Single-engine Fighter ( <i>Tempest V</i> ). A.R.C. Report 9253. September, 1945. (Unpublished.)
4.	S. Neumark, A. D. Young, and Miss Young	Result of a Step-by-Step Calculation of the Recovery of the <i>Typhoon</i> from a Terminal Velocity Dive. A.R.C. Report 7422. January, 1944. (Unpublished.)
5.	S. Neumark and Miss Young ..	A simplified Approach to the Problem of the Recovery of an Aeroplane from a High-Speed Dive with Constant Elevator Angle. A.R.C. Report 7423. January, 1944. (Unpublished.)
6.	B. Göthert .. .. ..	Effectiveness of a Spoiler at High Subsonic Speeds (Translation). M.O.S.(A) Volkenröde R. & T. No. 364. A.R.C. Report 11,172. February, 1947. (Unpublished.)

TABLE 1

*Notation*

$x_F$	Distance of flap hinge from leading edge (measured parallel to chord)
$c$	Chord of wing
$\phi$	Flap angle (measured from tangent at hinge line)
$\Delta C_L$	Increment of lift coefficient due to flap at constant incidence
$\Delta C_M$	Increment of pitching-moment coefficient due to flap at constant incidence
$C_{NF}$	Normal-force coefficient on flap
$C_{HF}$	Flap hinge-moment coefficient

TABLE 2

*Ordinates of NACA 0015 Section  
(Symmetrical)*

$(x/c)$	$(y/c)$
0	0
0.0125	0.02367
0.0250	0.03268
0.0500	0.04443
0.0750	0.05249
0.1000	0.05852
0.1500	0.06680
0.2000	0.07170
0.2500	0.07424
0.3000	0.07500
0.4000	0.07252
0.5000	0.06615
0.6000	0.05703
0.7000	0.04579
0.8000	0.03278
0.9000	0.01809
0.9500	0.01008
1.0000	0.00157

Leading-edge radius  $0.0248c$

TABLE 3

$\left(\frac{x}{c}\right)$ , Position of Pressure Holes

Lower Surface	Upper Surface
0.032	0.028
0.081	0.080
0.140	0.139
0.198	0.199
0.303	0.301
0.431	0.429
0.563	0.560
0.692	0.692
0.820	0.820
0.952	0.952

TABLE 4

Total Lift and Pitching-Moment Coefficients about Quarter-Chord Point

 $\alpha = 0 \text{ deg} ; \varphi = 40 \text{ deg}$ 

Case F $x_F/c = 0.205$			Case D $x_F/c = 0.308$			Case B $x_F/c = 0.404$		
$M$	$C_L$	$C_M$	$M$	$C_L$	$C_M$	$M$	$C_L$	$C_M$
0.741	0.783	-0.060	0.739	0.777	-0.063	0.741	0.744	-0.072
0.759	0.789	-0.102	0.759	0.824	-0.128	0.758	0.803	-0.130
0.781	0.728	-0.101	0.780	0.750	-0.119	0.780	0.731	-0.137
0.798	0.634	-0.089	0.798	0.658	-0.102	0.799	0.652	-0.116
0.811	0.565	-0.073	0.813	0.578	-0.079	0.820	0.559	-0.098

 $\alpha = 0 \text{ deg} ; \varphi = 20 \text{ deg}$ 

Case G $x_F/c = 0.204$			Case E $x_F/c = 0.309$			Case C $x_F/c = 0.395$		
$M$	$C_L$	$C_M$	$M$	$C_L$	$C_M$	$M$	$C_L$	$C_M$
0.742	0.462	-0.007	0.739	0.454	-0.010	0.740	0.405	-0.015
0.758	0.510	-0.028	0.761	0.535	-0.047	0.759	0.472	-0.041
0.782	0.589	-0.086	0.781	0.586	-0.090	0.781	0.552	-0.096
0.798	0.530	-0.088	0.799	0.526	-0.097	0.800	0.525	-0.112
0.817	0.435	-0.071	0.818	0.446	-0.086	0.820	0.363	-0.037

 $\alpha = 4 \text{ deg} ; \varphi = 40 \text{ deg}$ 

Case N $x_F/c = 0.205$			Case L $x_F/c = 0.308$			Case J $x_F/c = 0.404$		
$M$	$C_L$	$C_M$	$M$	$C_L$	$C_M$	$M$	$C_L$	$C_M$
0.741	0.764	-0.017	0.743	0.934	-0.051	0.742	0.992	-0.082
0.761	0.707	-0.014	0.762	0.881	-0.057	0.761	0.948	-0.088
0.782	0.675	-0.021	0.782	0.848	-0.062	0.779	0.892	-0.092
0.799	0.619	-0.025	0.797	0.812	-0.071	0.801	0.834	-0.103

 $\alpha = 4 \text{ deg} ; \varphi = 20 \text{ deg}$ 

Case P $x_F/c = 0.204$			Case M $x_F/c = 0.309$			Case K $x_F/c = 0.395$		
$M$	$C_L$	$C_M$	$M$	$C_L$	$C_M$	$M$	$C_L$	$C_M$
0.741	0.493	0.011	0.738	0.555	0.015	0.741	0.627	-0.001
0.761	0.452	0.010	0.761	0.535	0.006	0.761	0.603	-0.009
0.782	0.401	0.010	0.780	0.494	0.003	0.782	0.585	-0.021
			0.800	0.485	-0.008	0.799	0.550	-0.026

TABLE 5  
*Normal Force and Hinge-Moment Coefficients on Flap*

$\alpha = 0 \text{ deg} ; \varphi = 40 \text{ deg}$

Case F $x_F/c = 0.205$			Case D $x_F/c = 0.308$			Case B $x_F/c = 0.404$		
$M$	$C_{LF}$	$C_{MF}$	$M$	$C_{LF}$	$C_{MF}$	$M$	$C_{LF}$	$C_{MF}$
0.741	0.890	0.370	0.739	0.890	0.374	0.741	0.836	0.364
0.759	0.924	0.373	0.759	0.906	0.374	0.759	0.872	0.375
0.781	0.979	0.423	0.780	0.951	0.405	0.780	0.904	0.393
0.798	1.048	0.441	0.798	1.018	0.440	0.799	0.975	0.436
0.811	1.080	0.481	0.813	1.093	0.473	0.820	1.044	0.466

$\alpha = 0 \text{ deg} ; \varphi = 20 \text{ deg}$

Case G $x_F/c = 0.204$			Case E $x_F/c = 0.309$			Case C $x_F/c = 0.395$		
$M$	$C_{LF}$	$C_{MF}$	$M$	$C_{LF}$	$C_{MF}$	$M$	$C_{LF}$	$C_{MF}$
0.742	0.671	0.288	0.739	0.550	0.227	0.740	0.481	0.201
0.758	0.646	0.274	0.761	0.545	0.226	0.759	0.483	0.201
0.782	0.688	0.297	0.781	0.570	0.239	0.781	0.489	0.228
0.798	0.752	0.321	0.799	0.646	0.268	0.800	0.544	0.228
0.817	0.886	0.401	0.818	0.778	0.341	0.820	0.690	0.309

$\alpha = 4 \text{ deg} ; \varphi = 40 \text{ deg}$

Case N $x_F/c = 0.205$			Case L $x_F/c = 0.308$			Case J $x_F/c = 0.404$		
$M$	$C_{LF}$	$C_{MF}$	$M$	$C_{LF}$	$C_{MF}$	$M$	$C_{LF}$	$C_{MF}$
0.741	0.983	0.417	0.743	0.917	0.394	0.742	0.902	0.406
0.761	1.019	0.444	0.762	0.963	0.412	0.761	0.947	0.408
0.782	1.098	0.491	0.782	1.042	0.456	0.779	1.001	0.435
0.799	1.176	0.525	0.797	1.107	0.490	0.801	1.068	0.469

$\alpha = 4 \text{ deg} ; \varphi = 20 \text{ deg}$

Case P $x_F/c = 0.204$			Case M $x_F/c = 0.309$			Case K $x_F/c = 0.395$		
$M$	$C_{LF}$	$C_{MF}$	$M$	$C_{LF}$	$C_{MF}$	$M$	$C_{LF}$	$C_{MF}$
0.741	0.955	0.412	0.738	0.794	0.324	0.741	0.616	0.254
0.761	1.009	0.440	0.761	0.850	0.365	0.761	0.678	0.288
0.782	1.116	0.502	0.780	0.924	0.405	0.782	0.752	0.319
			0.800	1.089	0.496	0.799	0.816	0.354

TABLE 6  
*Pressure Coefficients. M = 0.76, α = 0 deg*

Position of Hole (x/c)	No Flap	φ = 40 deg			φ = 20 deg		
		$\left(\frac{x_F}{c}\right) = 0.404$	$\left(\frac{x_F}{c}\right) = 0.308$	$\left(\frac{x_F}{c}\right) = 0.205$	$\left(\frac{x_F}{c}\right) = 0.395$	$\left(\frac{x_F}{c}\right) = 0.309$	$\left(\frac{x_F}{c}\right) = 0.204$
		M = 0.759	M = 0.758	M = 0.759	M = 0.759	M = 0.759	M = 0.761
<i>Lower Surface</i>							
0.032	0.00	0.31	0.40	0.54	0.18	0.19	0.33
0.081	-0.49	-0.08	0.07	0.30	-0.27	-0.17	0.01
0.140	-0.73	-0.17	0.06	0.38	-0.43	-0.27	0.06
0.198	-0.91	-0.10	0.13	0.71	-0.39	-0.19	0.35
0.303	-1.05	0.23	0.72	-0.41	-0.12	0.39	-0.48
0.431	-0.94	-0.37	-0.40	-0.41	-0.34	-0.43	-0.50
0.563	-0.31	-0.38	-0.40	-0.42	-0.36	-0.43	-0.44
0.692	-0.18	-0.38	-0.41	-0.43	-0.37	-0.39	-0.39
0.820	-0.06	-0.39	-0.42	-0.43	-0.33	-0.33	-0.32
0.952	0.14	-0.40	-0.42	-0.42	-0.29	-0.28	-0.27
No. 1	No Flap	0.69	0.75	0.77	0.32	0.34	0.41
2		0.58	0.60	0.59	0.17	0.17	0.23
3		0.26	0.23	0.23	-0.01	-0.02	0.00
4		-0.37	-0.39	-0.40	-0.33	-0.40	-0.46
<i>Upper Surface</i>							
0.028	-0.10	-0.33	-0.38	-0.50	-0.26	-0.30	-0.36
0.080	-0.58	-0.75	-0.78	-0.84	-0.70	-0.74	-0.76
0.139	-0.80	-0.97	-0.99	-1.04	-0.91	-0.94	-0.97
0.199	-0.87	-1.04	-1.06	-1.11	-0.99	-1.02	-1.04
0.301	-1.00	-1.16	-1.18	-1.21	-1.11	-1.13	-1.15
0.429	-0.89	-1.22	-1.23	-1.25	-1.16	-1.19	-1.20
0.560	-0.28	-1.25	-1.28	-1.29	-1.09	-1.12	-1.13
0.692	-0.21	-1.17	-1.19	-1.21	-0.39	-0.71	-0.52
0.820	-0.06	-0.81	-1.03	-0.89	-0.26	-0.25	-0.26
0.952	0.14	-0.35	-0.38	-0.37	-0.25	-0.24	-0.24

TABLE 7  
*Pressure Coefficients. M = 0.76,  $\alpha = 4$  deg*

Position of Hole ( $x/c$ )	No Flap	$\phi = 40$ deg			$\phi = 20$ deg		
		$\left(\frac{x_F}{c}\right) = 0.404$	$\left(\frac{x_F}{c}\right) = 0.308$	$\left(\frac{x_F}{c}\right) = 0.205$	$\left(\frac{x_F}{c}\right) = 0.395$	$\left(\frac{x_F}{c}\right) = 0.309$	$\left(\frac{x_F}{c}\right) = 0.204$
		$M = 0.761$	$M = 0.761$	$M = 0.762$	$M = 0.761$	$M = 0.761$	$M = 0.761$
<i>Lower Surface</i>							
0.032	+0.41	0.62	0.68	0.73	0.51	0.52	0.56
0.081	-0.08	0.22	0.32	0.44	0.06	0.09	0.18
0.140	-0.35	0.08	0.22	0.45	-0.13	-0.08	0.13
0.198	-0.48	0.07	0.28	0.69	-0.19	-0.08	0.21
0.303	-0.57	0.21	0.78	-0.52	-0.08	0.37	-0.83
0.431	-0.52	-0.43	-0.47	-0.54	-0.53	-0.76	-0.78
0.563	-0.42	-0.44	-0.48	-0.54	-0.59	-0.69	-0.59
0.692	-0.27	-0.47	-0.49	-0.51	-0.50	-0.45	-0.39
0.820	-0.17	-0.47	-0.49	-0.46	-0.36	-0.28	-0.23
0.952	-0.04	-0.44	-0.45	-0.40	-0.22	-0.14	-0.12
No. 1	No Flap	0.74	0.72	0.76	0.36	0.36	0.46
2		0.60	0.62	0.62	0.18	0.15	0.23
3		0.26	0.34	0.23	-0.05	-0.08	-0.04
4		-0.43	-0.45	-0.51	-0.52	-0.71	-0.80
<i>Upper Surface</i>							
0.028	-0.62	-0.85	-0.89	-0.92	-0.75	-0.76	-0.76
0.080	-0.97	-1.10	-1.12	-1.11	-1.03	-1.04	-1.04
0.139	-1.19	-1.30	-1.31	-1.33	-1.24	-1.24	-1.25
0.199	-1.28	-1.39	-1.42	-1.39	-1.33	-1.33	-1.32
0.301	-1.25	-1.45	-1.46	-1.39	-1.39	-1.37	-1.28
0.429	-1.04	-1.48	-1.44	-1.25	-1.28	-1.16	-1.05
0.560	-0.58	-1.36	-1.25	-0.96	-0.81	-0.73	-0.68
0.692	-0.32	-0.94	-0.86	-0.73	-0.55	-0.49	-0.47
0.820	-0.12	-0.64	-0.65	-0.56	-0.32	-0.29	-0.29
0.952	0.02	-0.44	-0.46	-0.41	-0.17	-0.13	-0.13

TABLE 8

Pressure Coefficients.  $M = 0.80$ ,  $\alpha = 0$  deg

Position of Hole ( $x/c$ )	No Flap	$\phi = 40$ deg			$\phi = 20$ deg		
		$\left(\frac{x_F}{c}\right) = 0.404$	$\left(\frac{x_F}{c}\right) = 0.308$	$\left(\frac{x_F}{c}\right) = 0.205$	$\left(\frac{x_F}{c}\right) = 0.395$	$\left(\frac{x_F}{c}\right) = 0.309$	$\left(\frac{x_F}{c}\right) = 0.204$
		$M = 0.800$	$M = 0.799$	$M = 0.798$	$M = 0.798$	$M = 0.800$	$M = 0.799$
<i>Lower Surface</i>							
0.032	0.08	0.24	0.36	0.50	0.14	0.20	0.30
0.081	-0.40	-0.17	0.03	0.27	-0.32	-0.23	0.02
0.140	-0.63	-0.27	0.02	0.37	-0.53	-0.34	0.05
0.198	-0.81	-0.18	0.11	0.68	-0.52	-0.24	0.29
0.303	-0.97	0.21	0.72	-0.54	-0.08	0.38	-0.61
0.431	-1.01	-0.49	-0.52	-0.55	-0.40	-0.53	-0.62
0.563	-0.94	-0.50	-0.53	-0.55	-0.43	-0.51	-0.57
0.692	-0.32	-0.50	-0.53	-0.55	-0.42	-0.47	-0.47
0.820	-0.05	-0.50	-0.54	-0.55	-0.38	-0.42	-0.43
0.952	0.12	-0.51	-0.54	-0.53	-0.35	-0.38	-0.39
No. 1	No Flap	0.67	0.75	0.74	0.31	0.34	0.42
2		0.57	0.59	0.60	0.17	0.17	0.25
3		0.25	0.22	0.23	-0.02	-0.02	0.02
4		-0.48	-0.51	-0.53	-0.39	-0.49	-0.53
<i>Upper Surface</i>							
0.028	-0.04	-0.15	-0.22	-0.32	-0.10	-0.14	-0.17
0.080	-0.49	-0.58	-0.64	-0.68	-0.55	-0.55	-0.60
0.139	-0.72	-0.79	-0.84	-0.87	-0.76	-0.79	-0.81
0.199	-0.81	-0.88	-0.92	-0.95	-0.84	-0.87	-0.89
0.301	-0.94	-0.99	-1.03	-1.05	-0.99	-0.99	-1.01
0.429	-1.00	-1.07	-1.10	-1.11	-1.04	-1.06	-1.07
0.560	-0.94	-1.12	-1.15	-1.16	-1.08	-1.11	-1.11
0.692	-0.36	-1.06	-1.09	-1.10	-1.01	-1.04	-1.04
0.820	-0.04	-1.02	-1.06	-1.07	-0.87	-0.93	-0.95
0.952	0.12	-0.52	-0.56	-0.54	-0.29	-0.31	-0.34

TABLE 9  
*Pressure Coefficients. M = 0·8,  $\alpha = 4$  deg*

Position of Hole ( $x/c$ )	No Flap	$\phi = 40$ deg			$\phi = 20$ deg		
		$\left(\frac{x_F}{c}\right) = 0\cdot404$	$\left(\frac{x_F}{c}\right) = 0\cdot308$	$\left(\frac{x_F}{c}\right) = 0\cdot205$	$\left(\frac{x_F}{c}\right) = 0\cdot395$	$\left(\frac{x_F}{c}\right) = 0\cdot309$	$\left(\frac{x_F}{c}\right) = 0\cdot204$
		$M = 0\cdot799$	$M = 0\cdot801$	$M = 0\cdot797$	$M = 0\cdot799$	$M = 0\cdot799$	$M = 0\cdot800$
<i>Lower Surface</i>							
0·032	0·39	0·55	0·64	0·70	0·47	0·50	
0·081	-0·09	0·15	0·28	0·41	0·02	0·07	
0·140	-0·36	0	0·19	0·46	-0·19	-0·10	
0·198	-0·51	0·01	0·26	0·62	-0·24	-0·07	
0·303	-0·71	0·17	0·75	-0·70	-0·13	0·36	
0·431	-0·71	-0·58	-0·60	-0·73	-0·66	-0·98	
0·563	-0·80	-0·59	-0·61	-0·70	-0·70	-0·75	
0·692	-0·73	-0·60	-0·62	-0·65	-0·60	-0·55	
0·820	-0·20	-0·61	-0·61	-0·58	-0·48	-0·41	
0·952	-0·11	-0·59	-0·56	-0·51	-0·36	-0·29	
No. 1	No Flap	0·73	0·78	0·71	0·37	0·37	
2		0·59	0·63	0·63	0·19	0·19	
3		0·25	0·23	0·25	0·04	0·04	
4		-0·56	-0·57	-0·67	-0·65	-0·93	
<i>Upper Surface</i>							
0·028	-0·43	-0·58	-0·69	-0·70	-0·54	-0·57	
0·080	-0·79	-0·86	-0·93	-0·93	-0·85	-0·86	
0·139	-1·01	-1·07	-1·13	-1·13	-1·06	-1·07	
0·199	-1·09	-1·15	-1·22	-1·21	-1·16	-1·16	
0·301	-1·12	-1·24	-1·29	-1·28	-1·23	-1·24	
0·429	-0·99	-1·28	-1·33	-1·27	-1·19	-1·27	
0·560	-0·62	-1·31	-1·36	-1·18	-1·03	-1·05	
0·692	-0·42	-1·26	-1·28	-0·95	-0·72	-0·69	
0·820	-0·25	-0·95	-0·78	-0·70	-0·51	-0·44	
0·952	-0·09	-0·59	-0·53	-0·52	-0·34	-0·26	

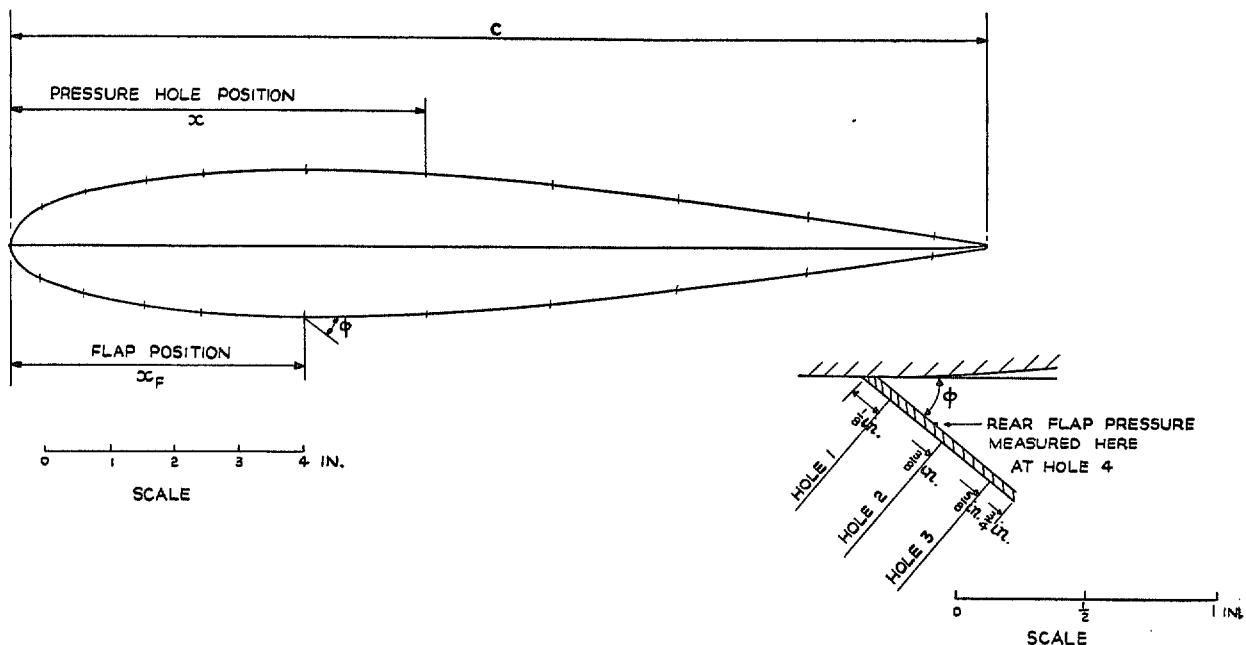


FIG. 1. Diagrams of aerofoil and flap.

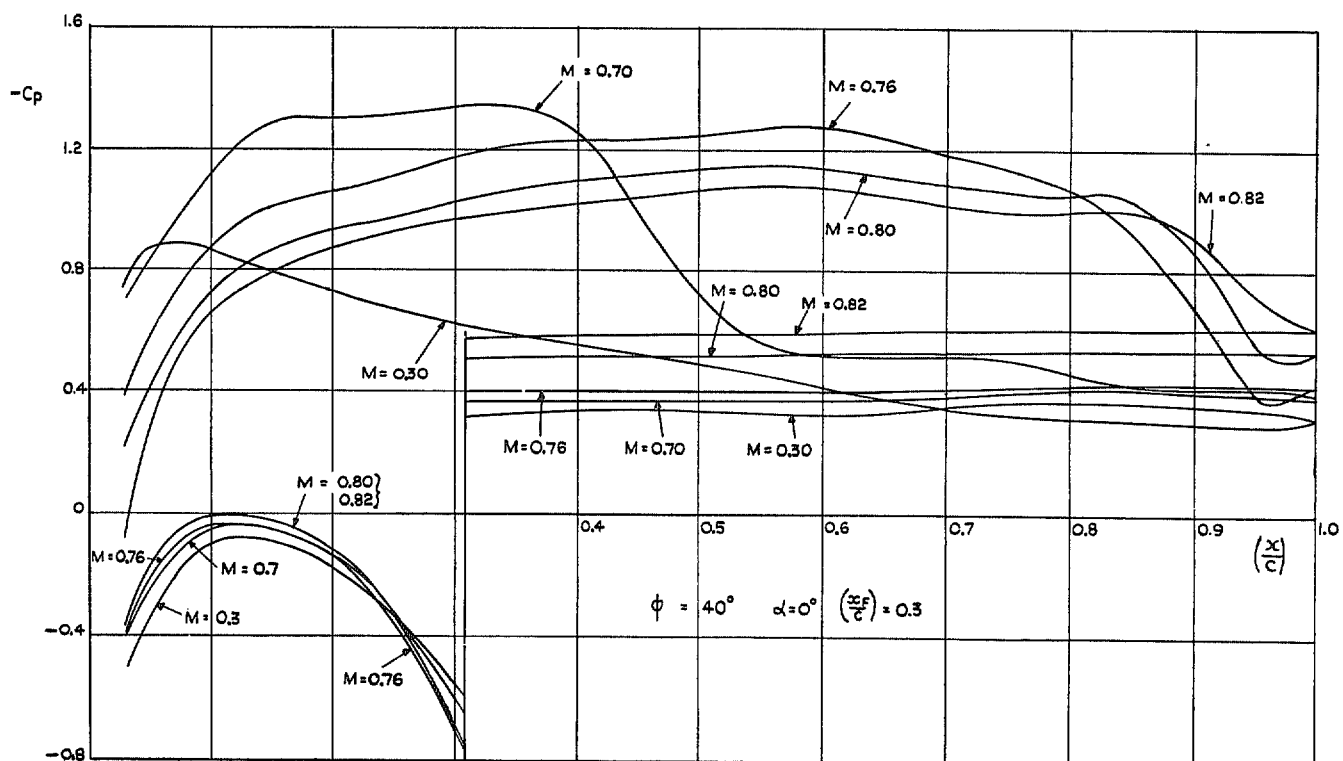


FIG. 2. Pressure distribution with flap. Effect of Mach number.

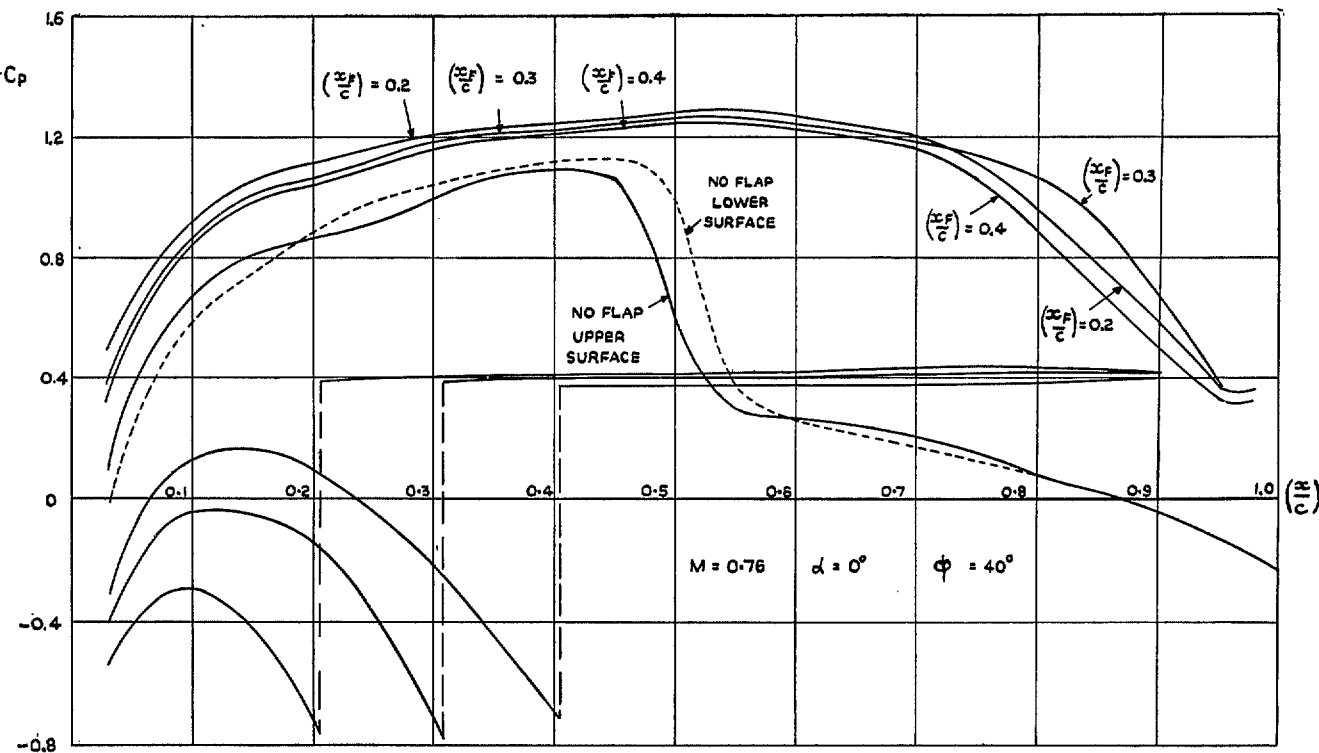


FIG. 3. Pressure distribution. Effect of flap position.

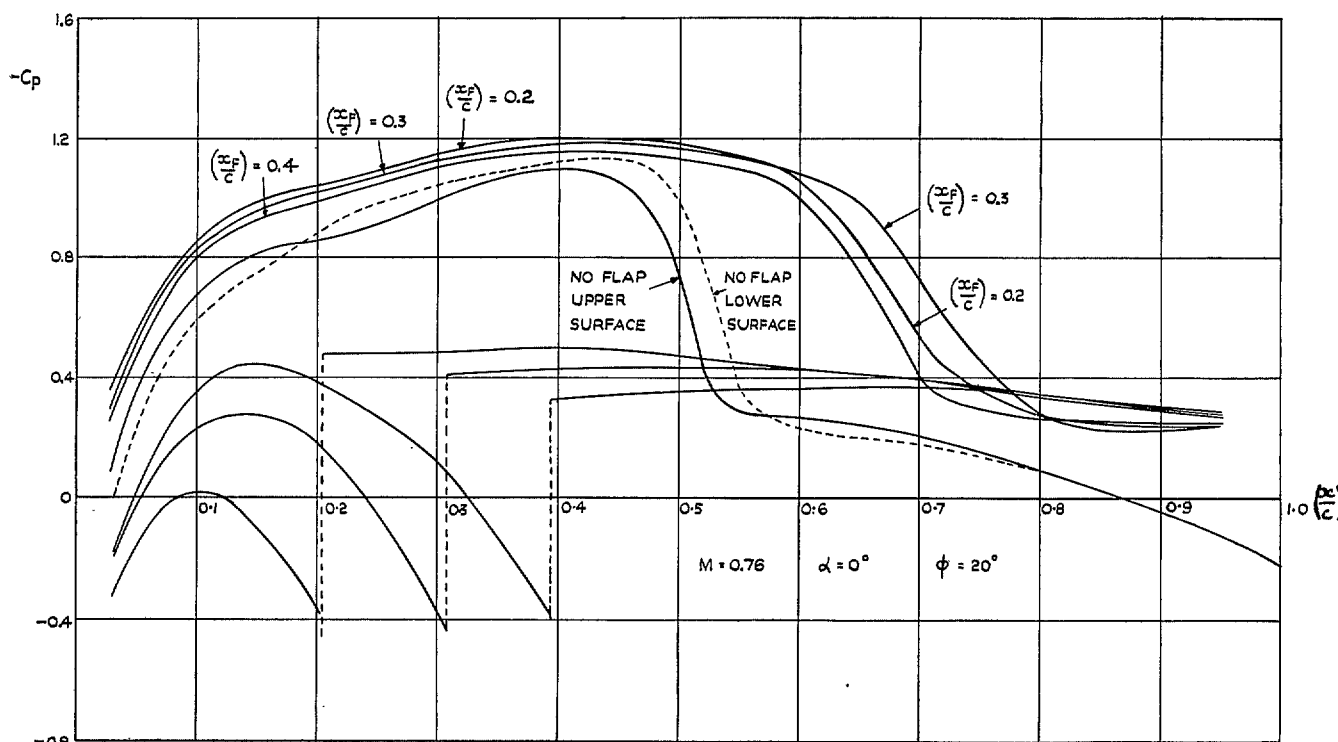


FIG. 4. Pressure distribution. Effect of flap position.

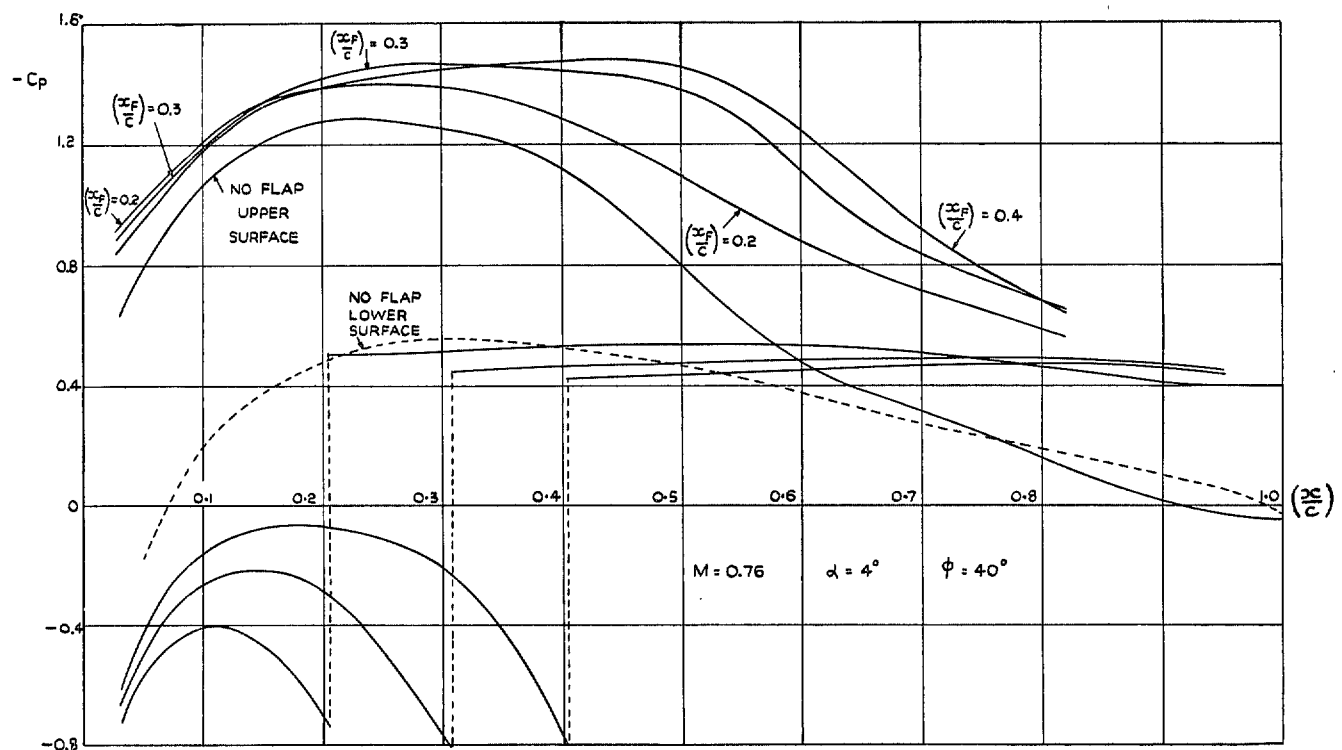


FIG. 5. Pressure distribution. Effect of flap position.

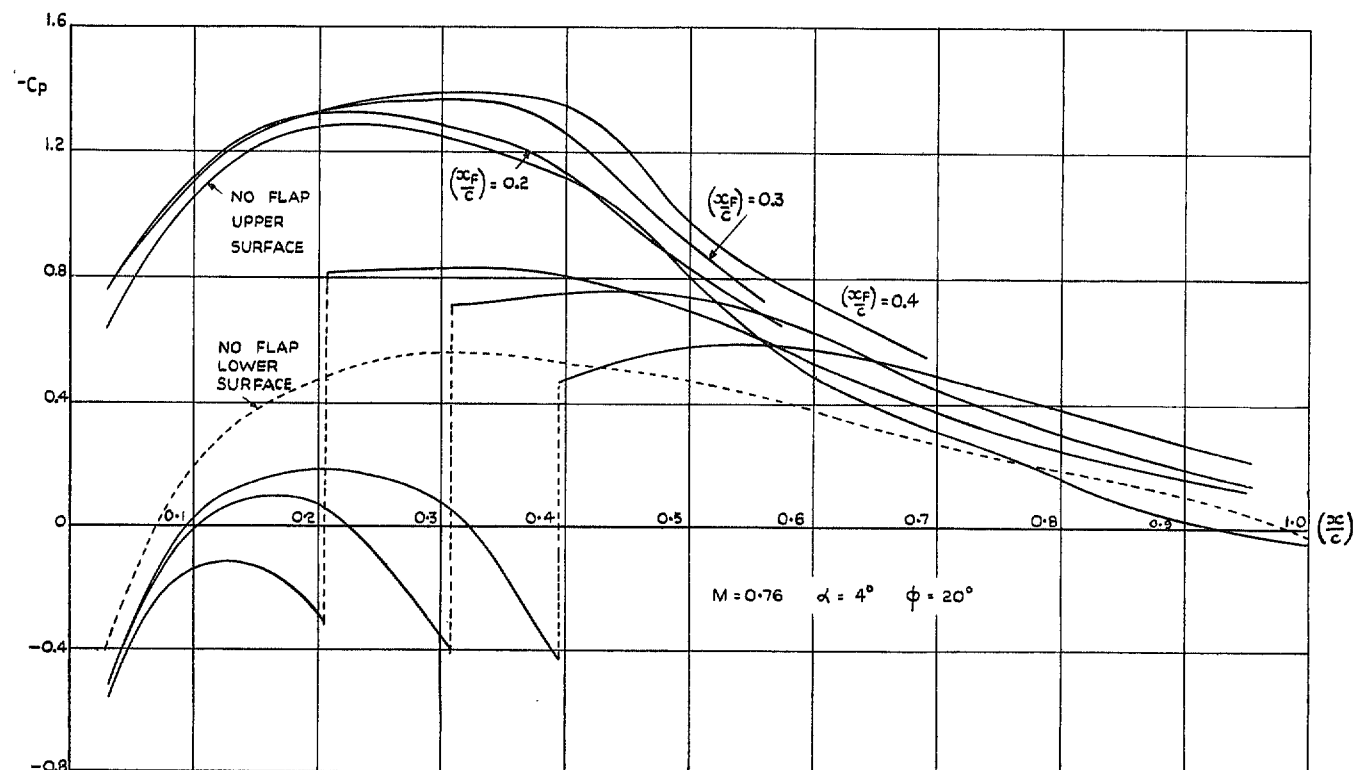


FIG. 6. Pressure distribution. Effect of flap position.

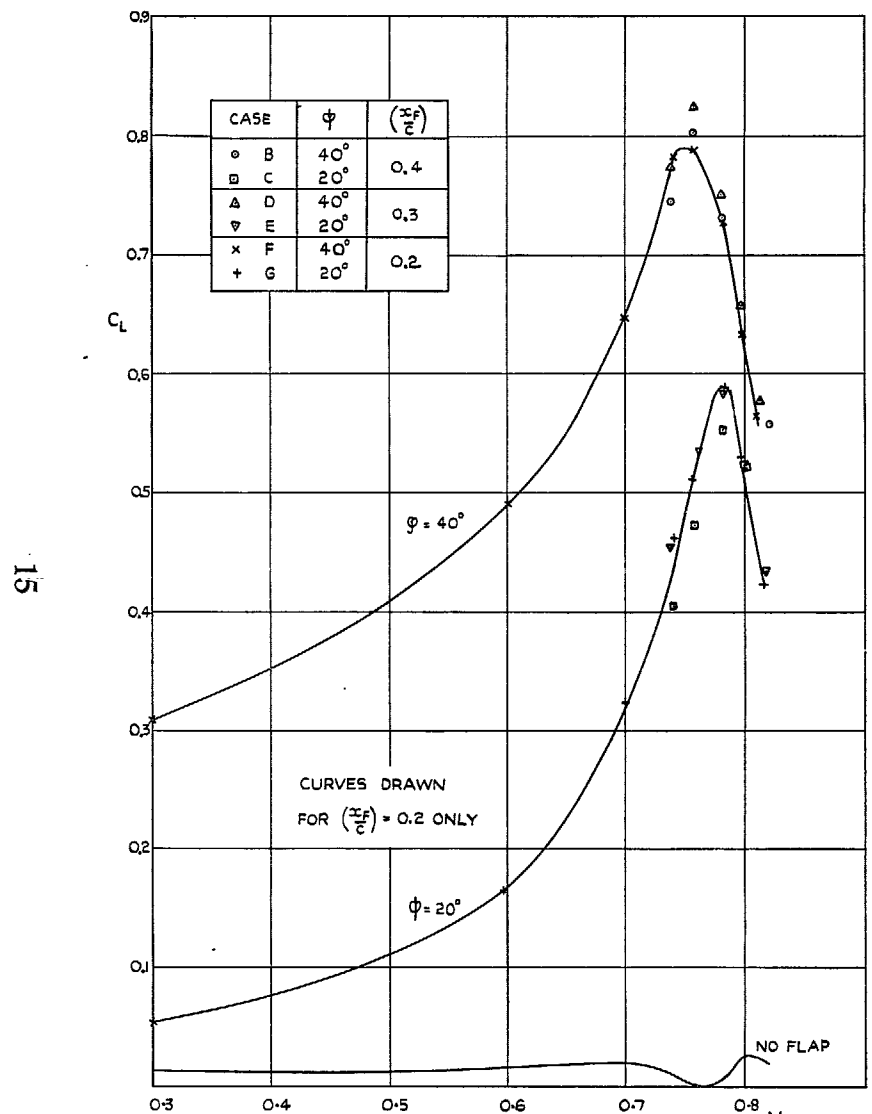


FIG. 7. Lift coefficients.  $\alpha = 0$  deg.

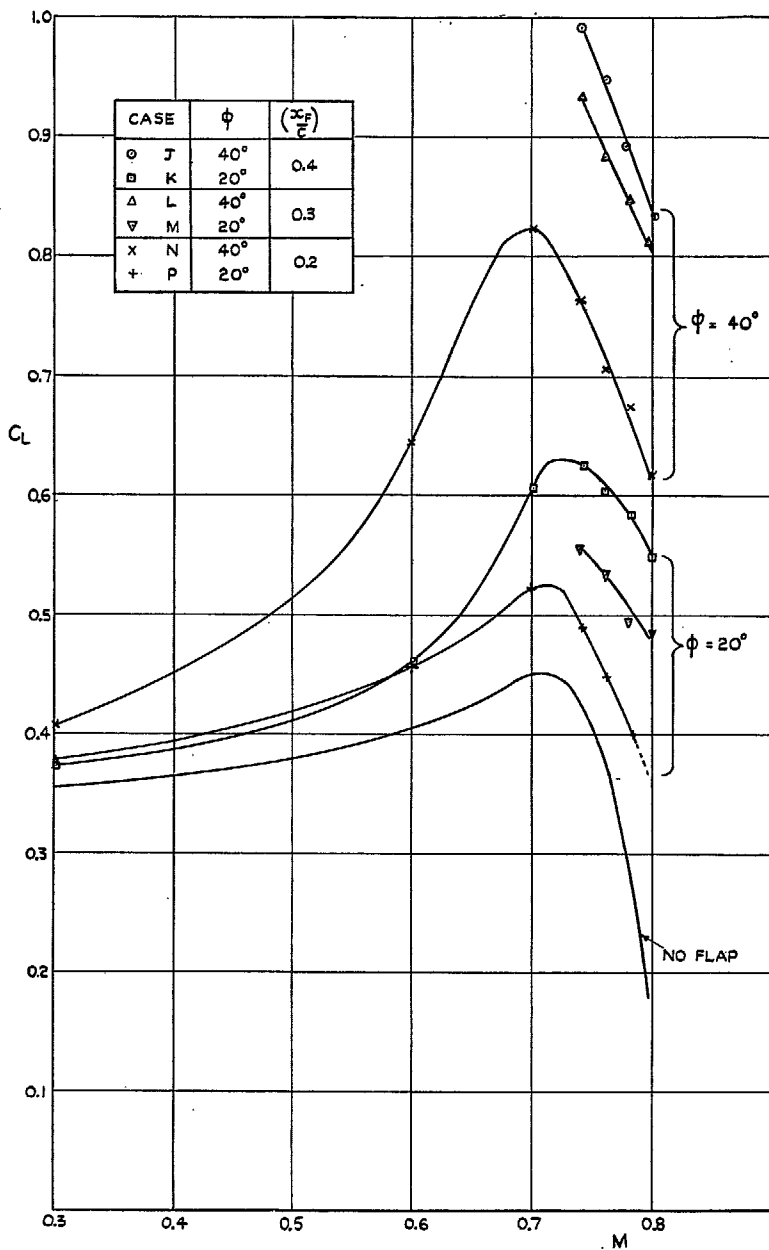


FIG. 8. Lift coefficients.  $\alpha = 4$  deg.

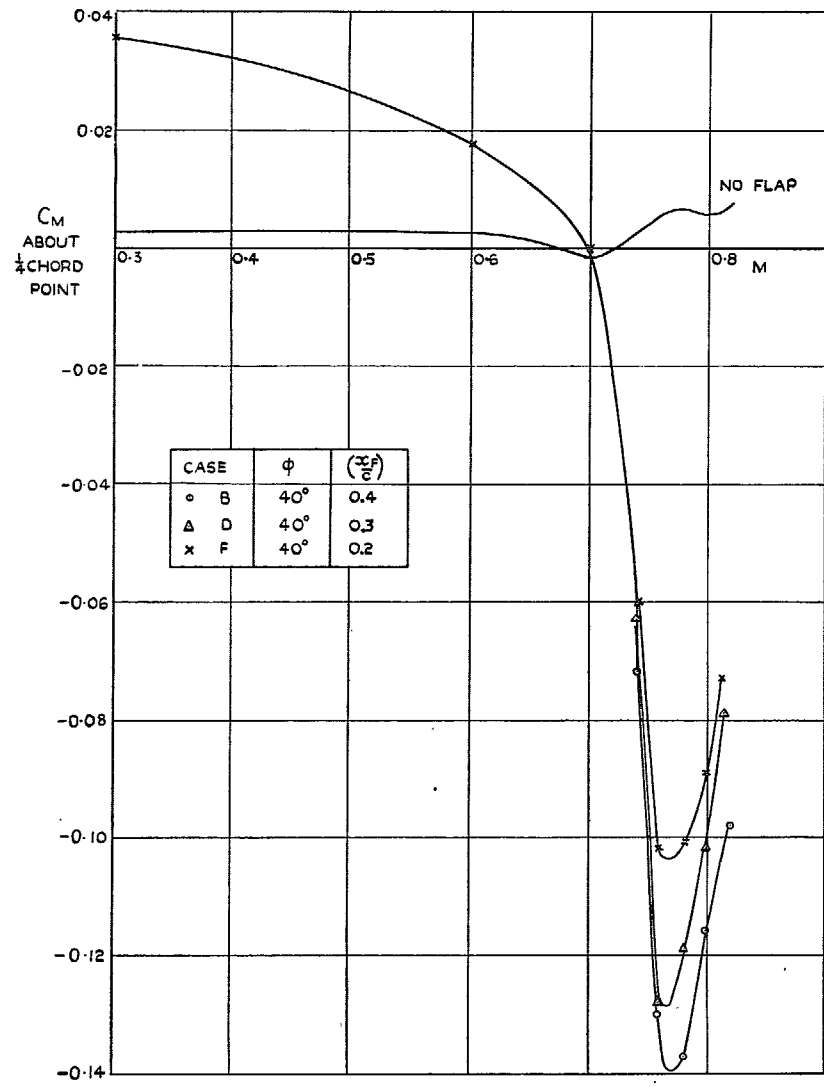


FIG. 9. Pitching-moment coefficients.  $\alpha = 0$  deg,  $\varphi = 40$  deg.

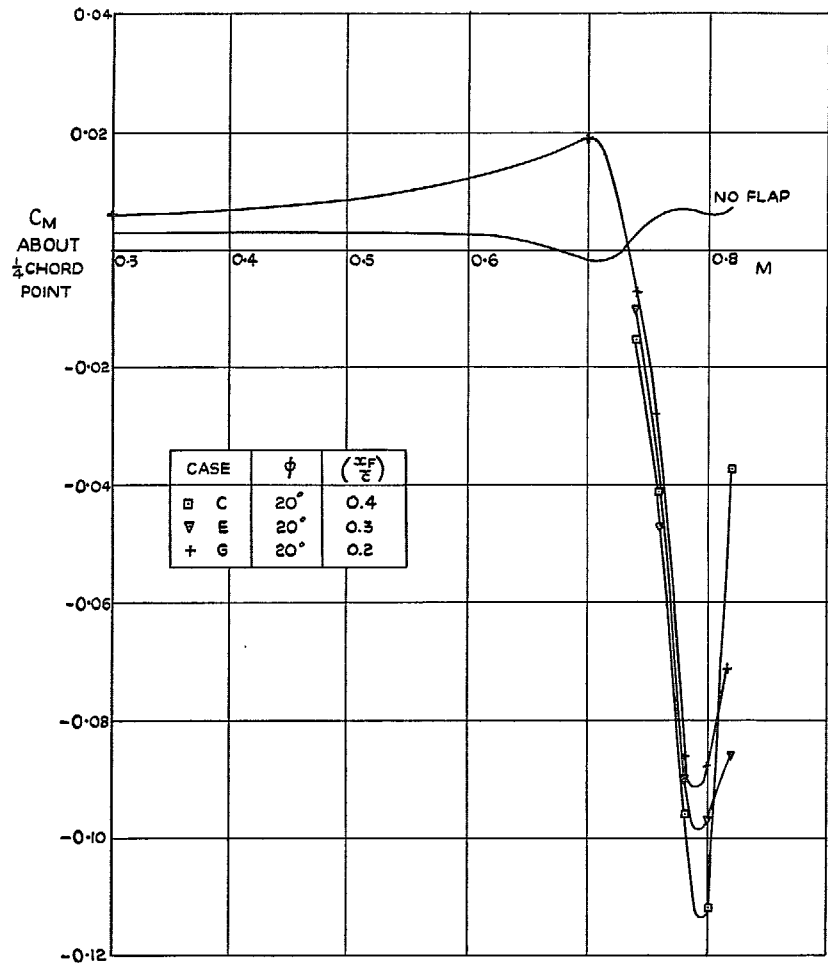


FIG. 10. Pitching-moment coefficients.  $\alpha = 0$  deg,  $\varphi = 20$  deg.

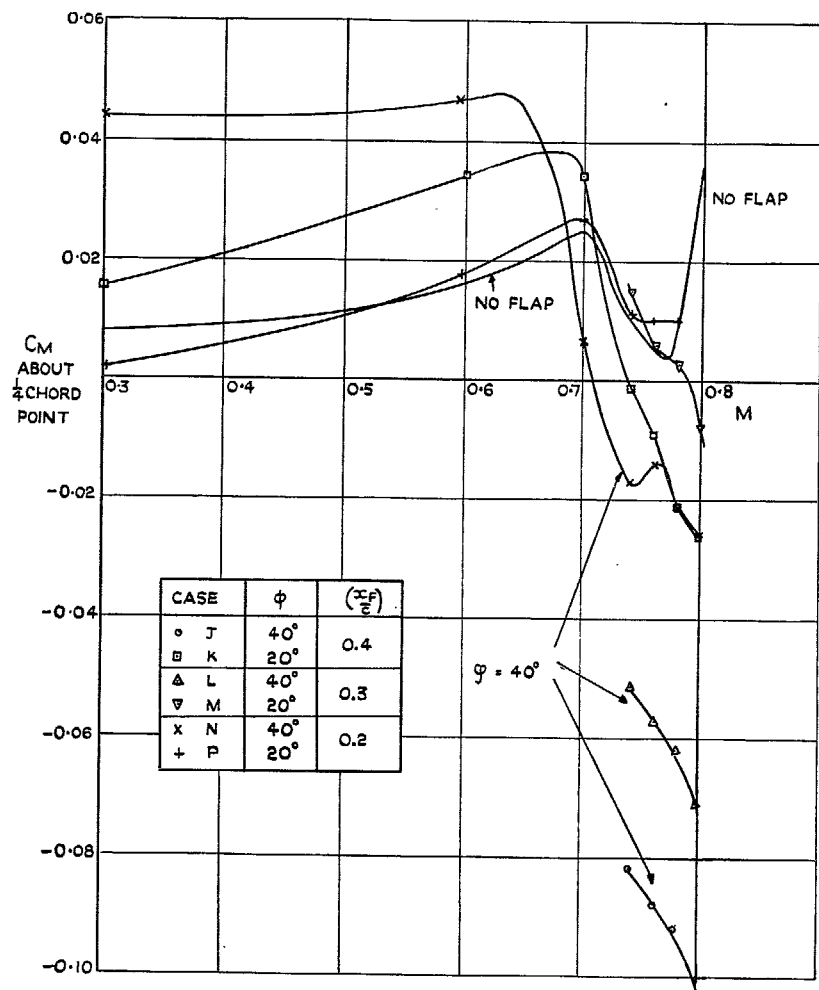


FIG. 11. Pitching-moment coefficients.  $\alpha = 4$  deg.

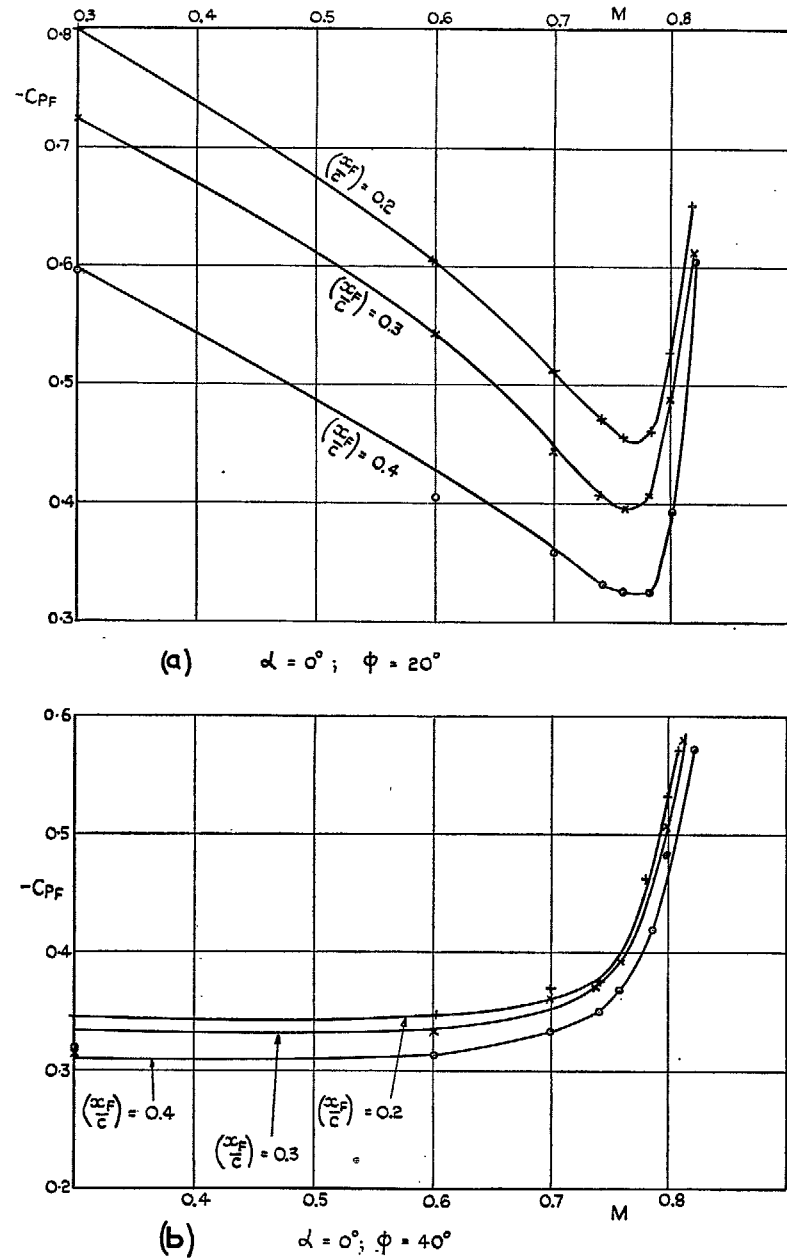


FIG. 12. Suction behind flap.

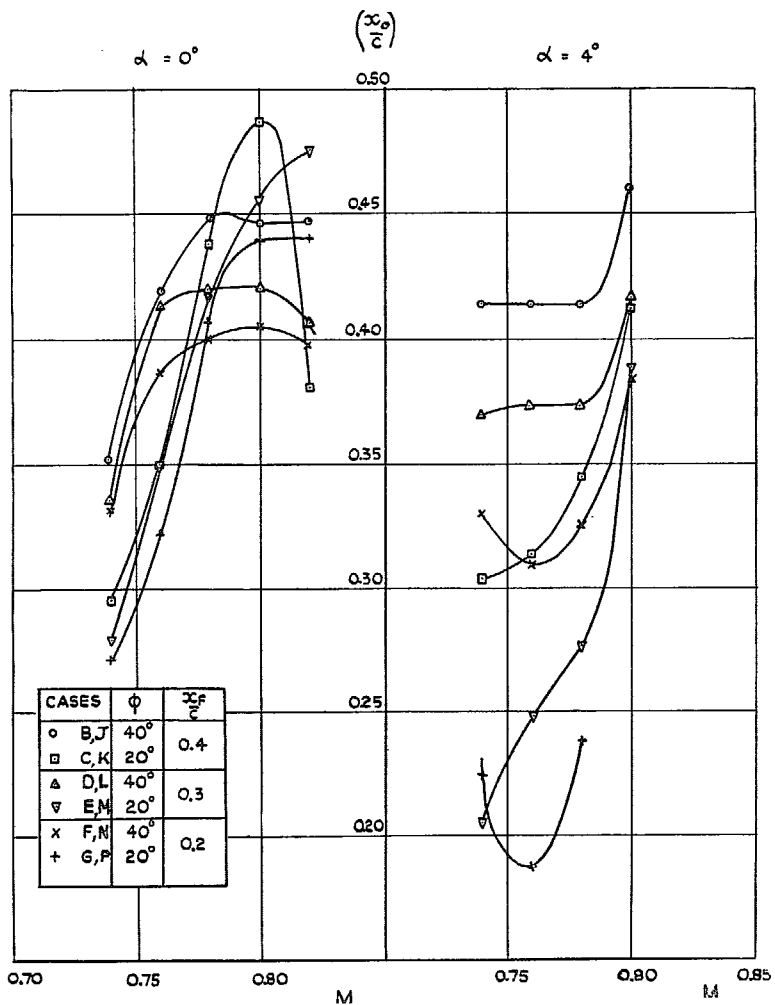


FIG. 13.

Chordwise position about which  $\Delta C_M = 0$ .

FIG. 14.

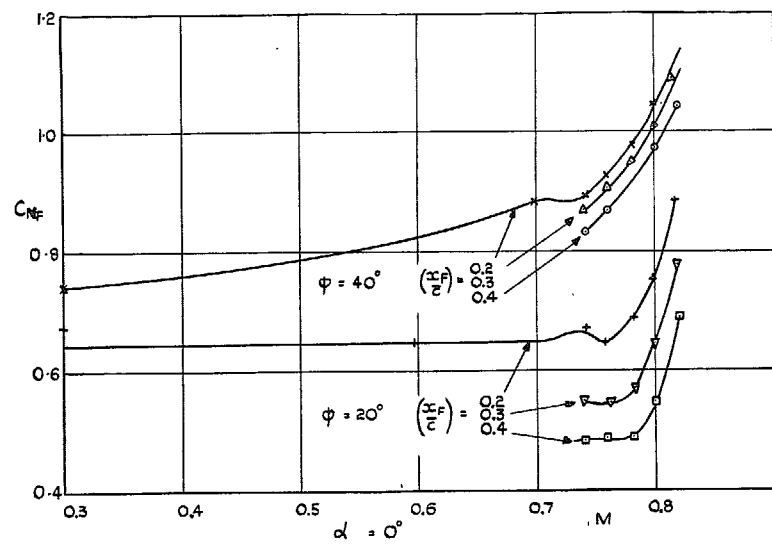


FIG. 15.

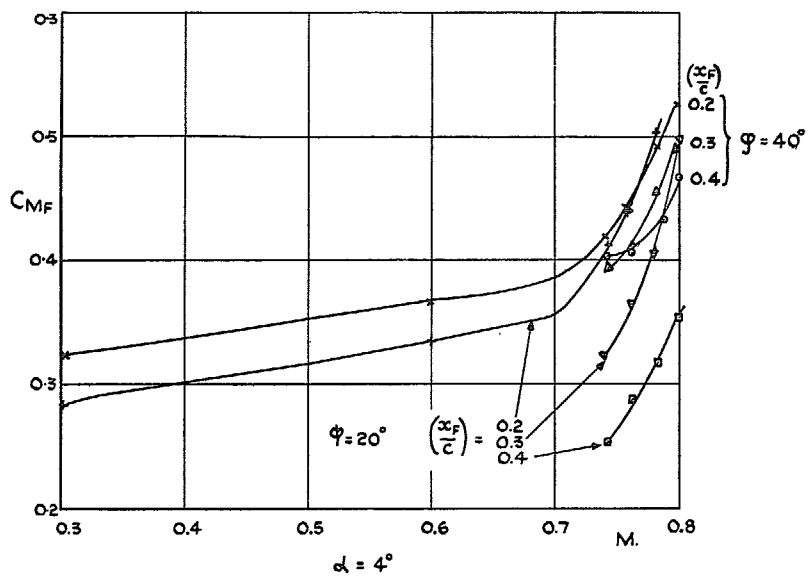


FIG. 16.

Flap forces.

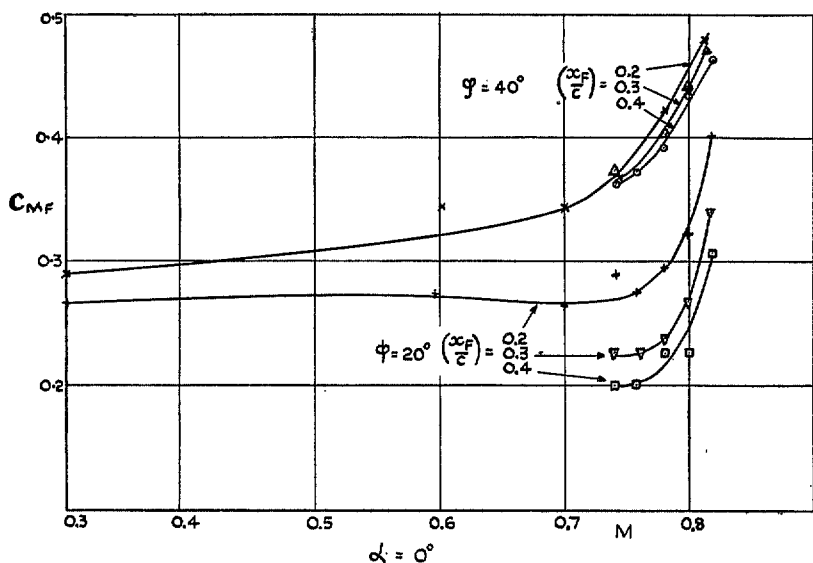


FIG. 17.

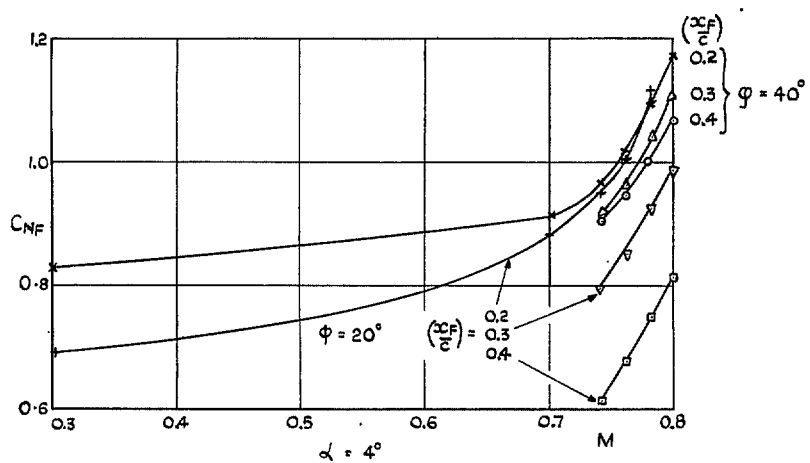


FIG. 18.  
Flap hinge moments.

## Publications of the Aeronautical Research Council

### ANNUAL TECHNICAL REPORTS OF THE AERONAUTICAL RESEARCH COUNCIL (BOUNDED VOLUMES)

- 1936 Vol. I. Aerodynamics General, Performance, Airscrews, Flutter and Spinning. 40s. (40s. 9d.)  
Vol. II. Stability and Control, Structures, Seaplanes, Engines, etc. 50s. (50s. 10d.)
- 1937 Vol. I. Aerodynamics General, Performance, Airscrews, Flutter and Spinning. 40s. (40s. 10d.)  
Vol. II. Stability and Control, Structures, Seaplanes, Engines, etc. 60s. (60s.)
- 1938 Vol. I. Aerodynamics General, Performance, Airscrews. 50s. (50s.)  
Vol. II. Stability and Control, Flutter, Structures, Seaplanes, Wind Tunnels, Materials. 30s. (30s. 9d.)
- 1939 Vol. I. Aerodynamics General, Performance, Airscrews, Engines. 50s. (50s. 11d.)  
Vol. II. Stability and Control, Flutter and Vibration, Instruments, Structures, Seaplanes, etc. 63s. (64s. 2d.)
- 1940 Aero and Hydrodynamics, Aerofoils, Airscrews, Engines, Flutter, Icing, Stability and Control, Structures, and a miscellaneous section. 50s. (50s.)
- 1941 Aero and Hydrodynamics, Aerofoils, Airscrews, Engines, Flutter, Stability and Control, Structures. 63s. (64s. 2d.)
- 1942 Vol. I. Aero and Hydrodynamics, Aerofoils, Airscrews, Engines. 75s. (76s. 3d.)  
Vol. II. Noise, Parachutes, Stability and Control, Structures, Vibration, Wind Tunnels. 47s. 6d. (48s. 5d.)
- 1943 Vol. I. (*In the press.*)  
Vol. II. (*In the press.*)

### ANNUAL REPORTS OF THE AERONAUTICAL RESEARCH COUNCIL—

1933-34	1s. 6d. (1s. 8d.)	1937	2s. (2s. 2d.)
1934-35	1s. 6d. (1s. 8d.)	1938	1s. 6d. (1s. 8d.)
April 1, 1935 to Dec. 31, 1936	4s. (4s. 4d.)	1939-48	3s. (3s. 2d.)

### INDEX TO ALL REPORTS AND MEMORANDA PUBLISHED IN THE ANNUAL TECHNICAL REPORTS, AND SEPARATELY—

April, 1950 - - - - R. & M. No. 2600. 2s. 6d. (2s. 7½d.)

### AUTHOR INDEX TO ALL REPORTS AND MEMORANDA OF THE AERONAUTICAL RESEARCH COUNCIL—

1909-1949. R. & M. No. 2570 15s. (15s. 3d.)

### INDEXES TO THE TECHNICAL REPORTS OF THE AERONAUTICAL RESEARCH COUNCIL—

December 1, 1936 — June 30, 1939.	R. & M. No. 1850.	1s. 3d. (1s. 4½d.)
July 1, 1939 — June 30, 1945	R. & M. No. 1950.	1s. (1s. 1½d.)
July 1, 1945 — June 30, 1946	R. & M. No. 2050.	1s. (1s. 1½d.)
July 1, 1946 — December 31, 1946.	R. & M. No. 2150.	1s. 3d. (1s. 4½d.)
January 1, 1947 — June 30, 1947.	R. & M. No. 2250.	1s. 3d. (1s. 4½d.)
July, 1951.	R. & M. No. 2350.	1s. 9d. (1s. 10½d.)

*Prices in brackets include postage.*

Obtainable from

### HER MAJESTY'S STATIONERY OFFICE

York House, Kingsway, London, W.C.2. 423 Oxford Street, London, W.1 (Post Orders:  
P.O. Box 569, London, S.E.1); 13a Castle Street, Edinburgh 2; 39, King Street, Manchester, 2;  
Edmund Street, Birmingham 3; 1 St. Andrew's Crescent, Cardiff; Tower Lane, Bristol 1;  
80 Chichester Street, Belfast, or through any bookseller